Polymer Chemistry

COMMUNICATION

Aspect-ratio-dependent interaction of molecular polymer brushes and multicellular tumour spheroids

Markus Müllner,[a,b,c,*] Kylie Yang,[a] Amandeep Kaur,[a] and Elizabeth J. New[a,c]

Received 00th January 20xx,
Accepted 00th January 20xx

DOI: 10.1039/x0xx00000x

www.rsc.org/

Polymer nanoparticles based on molecular polymer brushes allow precise and independent tailoring of nanoparticle characteristics. This enables the synthesis of soft hydrophilic polymer particles with matching composition and surface chemistry where only the aspect-ratio is varied. PEGylated brush nanoparticles revealed that brush nanorods exhibit higher association and penetration into multicellular tumour spheroids compared to their spherical or filamentous counterparts.

Nanoparticle-based carrier systems are expected to overcome many limitations of traditional delivery strategies for therapeutics and imaging diagnostics.[1] In particular, polymer nanoparticles are highly anticipated candidates for biomedical applications due to their flexible syntheses, avenues to various architectures and ease of incorporating specific functionalities. The past decades of research have established design guidelines regarding suitable particle properties (especially for size and surface chemistry) for *in vivo* applications. Closer investigation of nanoparticles at the interface with biological barriers has revealed the importance of shape on particle interaction and transport in cell tissues and tumours.[2] Cylindrical, in particular rod-like particles, have emerged as a new paradigm in nanomedicine. Rod- and worm-shaped nanomaterials have repeatedly demonstrated their potential to compete and outperform its spherical analogues.[2b] Most recently, rod-shaped amphiphilic block copolymer nanoparticles highlighted that particle shape may be used as a promising design criterion for polymeric drug delivery carriers.[3] In particular, their non-spherical shape (i.e. shape anisotropy) granted the nanoparticles exclusive access to cell nuclei. Dextran-coated magnetic nano-worms showed enhanced cell attachment and higher tumour targeting compared to spherical counterparts.[4] The shape effect is also evident in the observation that polyethylene glycol-*block*-polycaprolactone worm-like micelles exhibited different cellular interaction compared to spherical micelles of the same copolymer[5] and enhanced tumour shrinkage.[6] Virus nanoparticles have been reported for rod-shaped particles which have superior diffusion rates in spheroid models.[7] Nano-sized polystyrene rods showed faster cellular uptake kinetics compared to nanospheres of the same volume,[8] while PRINT® polymer nanogels of different shapes have shown favoured uptake for short rod-like particle geometries.[9] Similar trends are frequently observed for inorganic particles.[10]

Although shape anisotropy is often presented as an advantage in drug delivery applications, more studies are needed to affirm this assertion, as there are also a number of comparison studies ascribing benefits to spherical particles.[2b] This divergence in findings arises partially from the fact that some studies preclude direct comparison with polymer nano-systems as the investigation may have been performed using different types of cells or particles, or material composition.[11] Similarly, materials where multiple design parameters have been altered are difficult to interpret. For example, the production of differently-shaped gold nanomaterials can result in changes of both shape as well as surface chemistry.[12] While the 'shape effect' is acknowledged, its correlation to biological effects must be studied in more rigorous systematic studies to increase predictability and sustained development. A relatively small number of studies have explored shape-anisotropic polymeric nanomaterials as they remain challenging to produce. The effect of nanoparticle aspect ratio and topology on polymer particles is difficult to investigate due to the synthetic challenges in producing uniform nanomaterials with a defined aspect ratio and equal surface chemistry. A direct comparison between nanoparticle systems requires that ideally only one parameter is changed. To investigate and address this limitation, we used molecular polymer brushes (MPBs) to produce shape-anisotropic polymer nanoparticles and study

[a] School of Chemistry, The University of Sydney, Sydney 2006 NSW (Australia)
[b] Key Centre for Polymers and Colloids, The University of Sydney, Sydney 2006 NSW (Australia)
[c] The University of Sydney Nano Institute (Sydney Nano), Sydney 2006, NSW (Australia).
E-mail: markus.muellner@sydney.edu.au
Electronic Supplementary Information (ESI) available: Materials and experimental procedures, spectroscopy (NMR, fluorescence), SEC, cryo-TEM, AFM cross-sections and additional cell images. See DOI: 10.1039/x0xx00000x

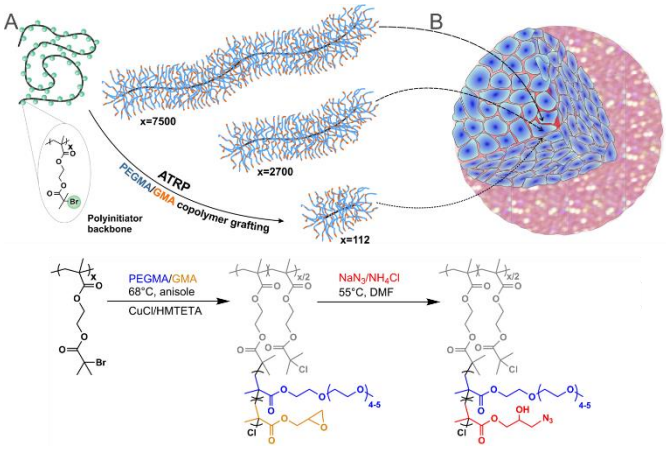

Figure 1. (Top) Molecular polymer brushes (MPBs) with different topology are produced via atom transfer radical polymerisation (ARTP) using the grafting-from approach on (A) a polyinitiator backbone with different molecular weights (x=repeat unit). (B) Post-functionalisation of the MPBs using fluorescent tags enabled to study the penetration of MPBs into multicellular tumour spheroids. (Bottom) Synthetic procedure to produce MPBs.

their association with multicellular tumour spheroids (MCS) (Figure 1). MPBs enable alteration of one parameter at a time while keeping other chemical or structural properties identical. In this way, it is possible to change the nanoparticle topology, shape or aspect ratio without affecting the chemical identity, such as composition, grafting density or surface properties. MPBs made from polyethylene glycol methyl ether methacrylate PEGMA were previously found to yield biologically relevant circulation half-lives and tumour accumulation in rodents.[13]

MPBs with different topology were prepared by varying the backbone length of MPBs while keeping side chain lengths the same. Recently, Cho *et al.* elegantly varied the topology of molecular brushes through the grafting through method at high pressures using PEGMA as macromonomers.[14] We opted to use 'grafting-from' to synthesise MPBs where the side chains are made from PEGMA. The synthetic strategy also eases the introduction of functionality into the side chains via copolymerisation.[13, 15] Different MPB topologies were obtained using poly(2-(2-bromoisobutyryloxy) ethyl methacrylate) (PBIEM) polyinitiator backbones of different degree of polymerisation (DP) to graft side chain of comparable DP. A detailed synthesis protocol for the PBIEM backbones has been previously described.[16] Copolymer brush side chains of PEGMA and glycidyl methacrylate (GMA) were grafted using atom transfer radical polymerisation (ATRP). The side chain length was calculated using proton nuclear magnetic resonance (^{1}HNMR), the monomer conversions and the reported grafting efficiency for PEGMA (~300 g·mol^{-1}). 'Grafting-from' typically compromises the grafting efficiency from PBIEM backbones due to the bulkiness of monomers and has been reported extensively.[17] We synthesised the following set of MPBs (Figure 1 and Table 1): spherical / ellipsoidal PBIEM$_{56}$-*co*-PBIEM$_{56}$-*graft*-[PEGMA$_{128}$-*co*-GMA$_{19}$] (**MPB-sphere**); rod-like PBIEM$_{1350}$-*co*-PBIEM$_{1350}$-*graft*-[PEGMA$_{90}$-*co*-GMA$_{12}$] (**MPB-rod**); and filament-like PBIEM$_{3750}$-*co*-PBIEM$_{3750}$-*graft*-[PEGMA$_{95}$-*co*-GMA$_{12}$] (**MPB-filament**). Cryogenic transmission electron microscopy (cryo-TEM) of the MPBs in water highlighted the transition from spherical/ellipsoidal to rod- and filament-like MPBs (Figure S1). The purified copolymer MPBs verified the incorporation of GMA into the brush structure (Figure S2). Reacting the epoxy ring of GMA with sodium azide was used to introduce further functionality into the brush architecture for subsequent copper-catalysed azide-alkyne cycloaddition (Cu-AAC). We used size exclusion chromatography (SEC) to investigate for brush-brush coupling. SEC revealed no intermolecular brush crosslinking after modification with sodium azide, as evident in the narrow distributions in the elution traces (Figure S3). As in our previous studies, we have used click chemistry to attach fluorescent tags to MPBs.[13] The successful attachment of Atto 488-alkyne was confirmed using fluorescence spectroscopy. Click chemistry allowed labelling the MPBs with similar amounts of fluorophores, confirmed by similar emission intensities of matching concentrations of aqueous brush solutions (1 g·L^{-1}) (Figure S4).

Table 1. Summary of PBIEM$_{x/2}$-*co*-PBIEM$_{x/2}$-*graft*-[PEGMA$_y$-*co*-GMA$_z$]$_{x/2}$ MPBs, including their observed topology and backbone length distribution.

MPB composition[a]	Topology	Backbone length[b] [nm]
PBIEM$_{56}$-*co*-PBIEM$_{56}$-*graft*-[PEGMA$_{128}$-*co*-GMA$_{19}$]	spherical/ ellipsoidal	40 ± 10
PBIEM$_{1350}$-*co*-PBIEM$_{1350}$-*graft*-[PEGMA$_{90}$-*co*-GMA$_{12}$]	rod-like	200 ± 60
PBIEM$_{3750}$-*co*-PBIEM$_{3750}$-*graft*-[PEGMA$_{95}$-*co*-GMA$_{12}$]	filamentous	1110 ± 210

[a] Calculated from ^{1}H NMR using 50% grafting efficiency of PEGMA from PBIEM backbones[17e]; [b] Determined from AFM height images using the *FiberApp*[18]

AFM confirmed the presence of individual polymer brush nanoparticles (Figure 2) and the morphology of the individual MPB systems. Keeping the length of the side chains similar and only varying the backbone length resulted in MPBs with altered

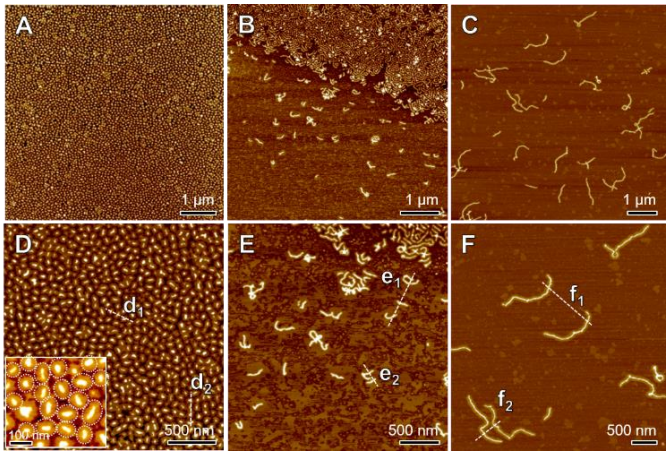

Figure 2. AFM height images of (A/D) MPB-sphere, (B/E) MPB-rod and (C/F) MPB-filament on freshly cleaved mica. Z-value is ± 3 nm in all images.

topology. The shortest MPB was sphere-like, as the side chains had a similar DP to the backbone (Figure 2A/D). Increasing the backbone length transitioned the MPBs into nanorods (Figure 2B/E) and filaments (Figure 2C/F). Cross-sectional analyses (dashed lines in Figure 2) confirmed comparable heights across the different MPB systems (Figure S5). Molecular brushes typically flatten on substrates during drying, resulting in side chains spreading and a decrease in height to only a few nanometres. All MPBs showed matching heights and comparable width in AFM, due to the identical synthesis protocol and homogeneous brushes, built-up via the 'grating-from' method. However, it is important to note that the real diameter of the brushes is difficult to estimate from AFM due to the flattening and tip convolution phenomena.

To assess the effects of polymer nanoparticle topology on the association and penetration of artificial tumours, we studied the interaction of MPBs with multicellular tumour spheroids (MCS) in 3D cell culture. Through the use of 3D cell cultures it is possible to mimic the complexity and heterogeneity of cancerous tumours more realistically *in vitro*.[19] MCS made from cancer cells are able to develop tumour characteristics, such as cell-cell interaction,[20] and establishing hypoxic regions[21] and an extracellular matrix.[22] We used DLD-1 colorectal adenocarcinoma cells, which yield uniform spherical MCSs (Figure 3A-C) and are a recommended epithelial cancer cell line adequate for future drug screening purposes.[23]

We used large MCS formed from 1×10^4 DLD-1 cells to study the topology-dependent association. Therefore, we incubated various concentrations of 488-labelled MPBs (0.1 – 10 $g\cdot L^{-1}$) with MCS for one day. Confocal laser scanning microscopy (CLSM) was used to generate z-stacks after imaging through individual MCS. Figure 3D-F depict an overlay of z-stacks of spheroids treated with MPB-spheres (D), MPB-rods (E) and MPB-filaments (F). The brighter the green colour, the more MPBs have associated with the individual MCS. Since the z-stack slice thickness, the incubation concentration, time, and the fluorophore content on the MPBs were kept constant, it was possible to directly compare the overlays. The rod-shaped MPBs associated to a higher extent with the spheroid surface compared to the sphere- and filament-like nanoparticles.

A similar trend was observed for the penetration into the spheroid (**Figure 3G-I**). An image slice through the centre of the MCS was used to qualitatively assess the ability of the various MPBs to penetrate the 3D cell tissue. We believe that the large MPB-filaments are too bulky to penetrate the spheroid. In contrast, rod-like MPBs could penetrate the spheroid tissue more effectively. We used ImageJ surface plots to highlight the homogenous penetration of rod-like MPBs comparted to their spherical and filamentous counterparts (Figure S6). Additional analysis using smaller MCS (formed from 5×10^3 DLD-1 cells) have confirmed this trend (Figure S7). While observations of the cellular interaction of nanoparticles differ in the literature (as described above), our results highlight the importance of shape (and aspect ratio) on the penetration of dense cellular aggregates, such as spheroids. Studying the interaction of the brush particles with DLD-1 in (2D) monolayers showed minimal association due to their PEGylated nature (Figure S8). Similar

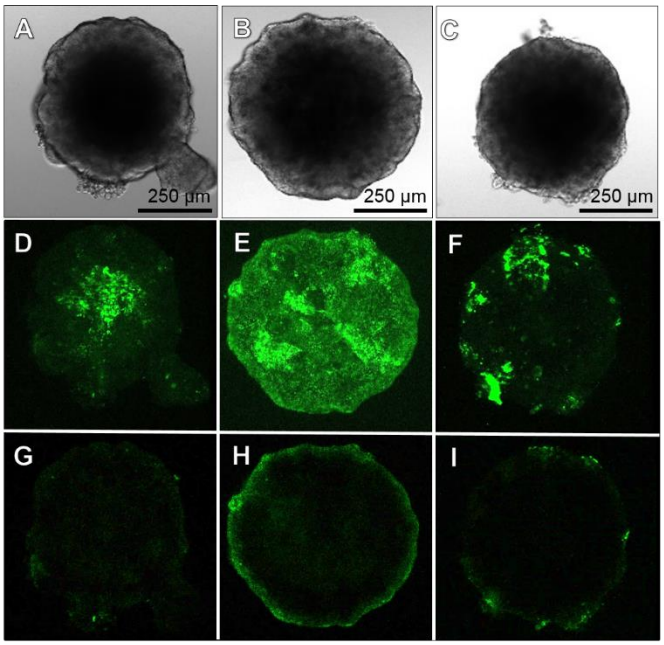

Figure 3. DIC images of DLD-1 MCS (A-C). CLSM z-stack (D-F) and mid-plane cross-section (G-I) to study the association and penetration of fluorescently labelled MPBs (green colour): (D/G) MPB-sphere, (E/H) MPB-rod and (F/I) MPB-filament. Details: MCS formed from 10,000 cells over 3 days; MPB concentration = 1.0 $g\cdot L^{-1}$; incubation time ~ 24 h.

trends have been observed using a macrophage cell line.[13a] Given the generically low cell association of PEGMA-based particles with cells, we assume that the spheroid penetration is largely dependent on diffusion processes. This in turn would explain the favourable penetration of rod-shaped particles, which has previously been reported for other nanorod systems.[24] Given that our MCS where incubated with identical MPB concentration also means that the individual MPB particle number in the MCS incubation is decreasing with increasing aspect ratio (i.e. increasing MPB molecular weight). We therefore ascribe the higher penetration of MPB-rods to a shape effect, as the same MCS (e.g. exposed to ~4 times higher number of MPB-spheres under identical conditions) showed much less penetration by the other MPB systems. Recently, favorable tumor penetration of MPBs and their advanced performance in the photothermal treatment of MCF-7 tumours *in vivo*[25] has been reported which further emphasises the importance of developing shape-anisotropic polymer nanoparticle systems.

Focussing on only rod-like MPBs, we studied the concentration dependence of the brush–spheroid interaction (Figure S9). Incubation with low concentrations of MPBs (0.25 $g\cdot L^{-1}$) resulted in low spheroid association and very limited penetration. With increasing concentration (0.5 and 1.0 $g\cdot L^{-1}$; i.e. increasing MPB particle number), the association also increased, and the penetration improved. The ability to finely tailor nanoparticle properties to affect their penetration capability, in combination with the shape effect and advantageous behaviour of non-spherical nanoparticles (e.g. margination, retention), may lead to new nanomedicines for *in vivo* applications, where the performance is not purely dictated by the surface chemistry of the drug carrier.

Conclusions

In summary, MPBs offer a straightforward methodology to produce polymer nanoparticles in which only one parameter is changed, independently. In the present study, the aspect ratio of the nanoparticles has been changed, allowing a direct comparison of the shape effect and investigating particles with identical composition and chemistries. An aspect ratio of ~4-5 gave rise to higher association to MCS and improved the penetration capabilities of the nanoparticles into the centre of the spheroid. To assess opportunities to translate our findings to drug delivery, we are currently studying the mechanism by which the particles penetrate and diffuse into the MCS. Recent studies highlighted the preferential association and penetration of, for example, rod-like virus particles,[26] elongated micelles,[5] and inorganic nanorods.[24] Here we have shown that MPBs are following this trend and anticipate that the ability to alter the particle design parameter independently will provide the opportunity to better correlate the shape effect to the nanoparticle performance, and contribute to the development of advanced drug carrier systems.

Conflicts of interest

There are no conflicts to declare.

Acknowledgements

This work was funded through an ARC Discovery Early Career Researcher Award (DE180100007). M.M. acknowledges support from the Faculty of Science (University of Sydney) Seed funding scheme, the Selby Research Foundation, and the Australian Nanotechnology Network Overseas Travel Fellowship. A.K. thanks the University of Sydney for a World Scholars Scholarship and the John A. Lamberton Research Scholarship. K.Y thanks the Australian government for an Australian Postgraduate Award. E.J.N. thanks the Westpac Bicentennial Foundation for a Research Fellowship. This work made use of the Aalto University Nanomicroscopy Center (Aalto-NMC) premises. The authors thank A/Prof Chiara Neto for access to instrumentation and acknowledge the scientific and technical assistance from the Australian Centre for Microscopy and Microanalysis staff at the University of Sydney.

Notes and references

1. a) S. Behzadi, V. Serpooshan, W. Tao, M. A. Hamaly, M. Y. Alkawareek, E. C. Dreaden, D. Brown, A. M. Alkilany, O. C. Farokhzad and M. Mahmoudi, *Chem. Soc. Rev.*, 2017, **46**, 4218-4244; b) R. A. Petros and J. M. DeSimone, *Nat Rev Drug Discov*, 2010, **9**, 615-627.
2. a) A. E. Nel, L. Madler, D. Velegol, T. Xia, E. M. V. Hoek, P. Somasundaran, F. Klaessig, V. Castranova and M. Thompson, *Nat Mater*, 2009, **8**, 543-557; b) S. Venkataraman, J. L. Hedrick, Z. Y. Ong, C. Yang, P. L. R. Ee, P. T. Hammond and Y. Y. Yang, *Adv. Drug Deliv. Rev.*, 2011, **63**, 1228-1246; c) N. P. Truong, M. R. Whittaker, C. W. Mak and T. P. Davis, *Expert Opin. Drug Deliv.*, 2015, **12**, 129-142; d) S. Barua and S. Mitragotri, *Nano Today*, 2014, **9**, 223-243.
3. E. Hinde, K. Thammasiraphop, H. T. T. Duong, J. Yeow, B. Karagoz, C. Boyer, J. J. Gooding and K. Gaus, *Nat Nano*, 2017, **12**, 81-89.
4. J.-H. Park, G. von Maltzahn, L. Zhang, M. P. Schwartz, E. Ruoslahti, S. N. Bhatia and M. J. Sailor, *Adv. Mater.*, 2008, **20**, 1630-1635.
5. Y. Geng, P. Dalhaimer, S. Cai, R. Tsai, M. Tewari, T. Minko and D. E. Discher, *Nat Nano*, 2007, **2**, 249.
6. D. A. Christian, S. Cai, O. B. Garbuzenko, T. Harada, A. L. Zajac, T. Minko and D. E. Discher, *Mol. Pharm.*, 2009, **6**, 1343-1352.
7. K. L. Lee, L. C. Hubbard, S. Hern, I. Yildiz, M. Gratzl and N. F. Steinmetz, *Biomater. Sci.*, 2013, **1**, 581-588.
8. A. Banerjee, J. Qi, R. Gogoi, J. Wong and S. Mitragotri, *J. Contr. Release*, 2016, **238**, 176-185.
9. S. E. A. Gratton, P. A. Ropp, P. D. Pohlhaus, J. C. Luft, V. J. Madden, M. E. Napier and J. M. DeSimone, *Proc. Natl Acad. Sci.*, 2008, **105**, 11613-11618.
10. H. Meng, S. Yang, Z. Li, T. Xia, J. Chen, Z. Ji, H. Zhang, X. Wang, S. Lin, C. Huang, Z. H. Zhou, J. I. Zink and A. E. Nel, *ACS Nano*, 2011, **5**, 4434-4447.
11. a) N. Doshi, B. Prabhakarpandian, A. Rea-Ramsey, K. Pant, S. Sundaram and S. Mitragotri, *J. Contr. Release*, 2010, **146**, 196-200; b) P. Decuzzi, B. Godin, T. Tanaka, S. Y. Lee, C. Chiappini, X. Liu and M. Ferrari, *J. Contr. Release*, 2010, **141**, 320-327; c) Y. Qiu, Y. Liu, L. Wang, L. Xu, R. Bai, Y. Ji, X. Wu, Y. Zhao, Y. Li and C. Chen, *Biomater.*, 2010, **31**, 7606-7619.
12. Arnida, A. Malugin and H. Ghandehari, *J. Appl. Toxicol.*, 2010, **30**, 212-217.
13. a) M. Müllner, S. J. Dodds, T.-H. Nguyen, D. Senyschyn, C. J. H. Porter, B. J. Boyd and F. Caruso, *ACS Nano*, 2015, **9**, 1294-1304; b) M. Müllner, D. Mehta, C. J. Nowell and C. J. H. Porter, *Chem. Comm.*, 2016, **52**, 9121-9124.
14. H. Y. Cho, P. Krys, K. Szcześniak, H. Schroeder, S. Park, S. Jurga, M. Buback and K. Matyjaszewski, *Macromolecules*, 2015, **48**, 6385-6395.
15. T. Pelras, H. T. T. Duong, B. J. Kim, B. S. Hawkett and M. Müllner, *Polymer*, 2017, **112**, 244-251.
16. a) M. Zhang, T. Breiner, H. Mori and A. H. E. Müller, *Polymer*, 2003, **44**, 1449-1458; b) M. Müllner, T. Lunkenbein, J. Breu, F. Caruso and A. H. E. Müller, *Chem. Mater.*, 2012, **24**, 1802-1810.
17. a) B. S. Sumerlin, D. Neugebauer and K. Matyjaszewski, *Macromolecules*, 2005, **38**, 702-708; b) Y. Xu, S. Bolisetty, M. Drechsler, B. Fang, J. Yuan, M. Ballauff and A. H. E. Müller, *Polymer*, 2008, **49**, 3957-3964; c) Y. Xu, J. Yuan and A. H. E. Müller, *Polymer*, 2009, **50**, 5933-5939; d) S. Y. Yu-Su, S. S. Sheiko, H.-i. Lee, W. Jakubowski, A. Nese, K. Matyjaszewski, D. Anokhin and D. A. Ivanov, *Macromolecules*, 2009, **42**, 9008-9017; e) Z. Zheng, M. Müllner, J. Ling and A. H. E. Müller, *ACS Nano*, 2013, **7**, 2284-2291.
18. I. Usov and R. Mezzenga, *Macromolecules*, 2015, **48**, 1269-1280.
19. K. M. Yamada and E. Cukierman, *Cell*, 2007, **130**, 601-610.
20. B. M. Baker and C. S. Chen, *J. Cell Sci.*, 2012, **125**, 3015-3024.
21. G. Mehta, A. Y. Hsiao, M. Ingram, G. D. Luker and S. Takayama, *J. Contr. Release*, 2012, **164**, 192-204.
22. L. C. Kimlin, G. Casagrande and V. M. Virador, *Mol. Carcinogen.*, 2013, **52**, 167-182.
23. J. Friedrich, C. Seidel, R. Ebner and L. A. Kunz-Schughart, *Nat. Protocols*, 2009, **4**, 309-324.
24. V. P. Chauhan, Z. Popović, O. Chen, J. Cui, D. Fukumura, M. G. Bawendi and R. K. Jain, *Angew. Chem. Int. Ed.*, 2011, **50**, 11417-11420.
25. H. Li, H. Liu, T. Nie, Y. Chen, Z. Wang, H. Huang, L. Liu and Y. Chen, *Biomater.*, 2018, DOI: 10.1016/j.biomaterials.2018.03.032.

26. P. L. Chariou, K. L. Lee, J. K. Pokorski, G. M. Saidel and N. F. Steinmetz, *J. Phys. Chem. B*, 2016, **120**, 6120-6129.